Phase transitions and thermal properties of decamethylferrocenium salts with perfluoroalkyl-sulfonate and -carboxylate anions exhibiting disorder

Hamada, Shota
Funasako, Yusuke
Mochida, Tomoyuki
Kuwahara, Daisuke
Yoza, Kenji

(Citation)
Journal of Organometallic Chemistry,713:35-41

(Issue Date)
2012-08-15

(Resource Type)
journal article

(Version)
Accepted Manuscript

(URL)
https://hdl.handle.net/20.500.14094/90001813

Phase transitions and thermal properties of decamethylferrocenium salts with perfluoroalkyl-sulfonate and -carboxylate anions exhibiting disorder

Shota Hamada[a], Yusuke Funasako[a], Tomoyuki Mochida[a,*], Daisuke Kuwahara[b], and Kenji Yoza[c]

[a]*Department of Chemistry, Graduate School of Science, Kobe University, Kobe, Hyogo 657-8501, Japan,*

[b]*The University of Electro-Communications, Chofu, Tokyo 182-8585, Japan*

[c]*Bruker AXS K.K., Moriya, Kanagawa, Yokohama, Kanagawa 221-0022, Japan*

Abstract

Decamethylferrocenium salts with perfluoroalkylsulfonate anions ($C_nF_{2n+1}SO_3^-$; n = 1, 4, and 8) and perfluoroalkylcarboxylate anions ($C_nF_{2n+1}CO_2^-$; n = 1–4) were prepared to investigate the effects of the anion on the thermal behaviors of the salts. Differential scanning calorimetry (DSC) measurements revealed that all the salts exhibited phase transitions in the solid state. Salts with an octamethylferrocenium cation or decamethylcobaltocenium cation exhibited different phase sequences from those of the corresponding decamethylferrocenium salts. Structural changes associated with the phase transitions were investigated crystallographically for two salts. The phase transition in $[Fe(C_5Me_5)_2](CF_3SO_3)$ at −121.6 °C was accompanied by ordering of the cation conformations into eclipsed and staggered conformations in different ratios. The unit-cell volume became six times larger and the space group changed from Pmn2_1 to P1 in the low-temperature phase. The phase transition in $[Fe(C_5Me_5)_2](C_3F_7CO_2)$ at −115 °C was not accompanied by any change in the unit cell or the space group ($P2_1$/c). The libration or displacements of the anions that existed in the high-temperature phase was suppressed in the low-temperature phase, associated with a slight rotational displacement of the molecules. Anions with longer perfluoroalkyl chains exhibited disorder in the solid state even at low temperatures.

Keywords: Decamethylferrocene; Perfluoroalkylcarboxylate; Perfluoroalkylsulfonate; Crystal

structure; Phase transition; Order-disorder

---

*Corresponding Author. Tel/Fax: +81-78-803-5679

E-mail: tmochida@platinum.kobe-u.ac.jp (T. Mochida)

1. Introduction

Metallocenium salts often exhibit phase transitions in the solid state, and these transitions are frequently associated with changes in molecular motion [1]. This tendency is partly ascribed to their nearly spherical molecular shapes. The simplest example is ferrocenium hexafluorophosphate, which exhibits a phase transition to an orientationally disordered phase at 74 °C, as shown by calorimetry, solid-state NMR, and X-ray crystallography [2]. Mössbauer spectroscopy has also been used to investigate molecular motion in ferrocenium salts [3]. Phase transitions in cobaltocenium derivatives and related compounds have been investigated extensively [4].

We have investigated phase-transition phenomena in ferrocene-based compounds, such as electronic phase-transitions [5] and order–disorder transitions [6]. Recently, we prepared metallocenium salts with trifluoromethanesulfonamide [7]; these salts are ionic liquids with melting points below 100 °C [8]. In this context, we became interested in thermal properties such as melting points and phase transitions in metallocenium salts with fluorinated anions. In this paper, we report the thermal properties of the metallocenium salts shown in Chart 1; decamethylferrocenium ($[FeCp^*_2]^+$) salts with perfluoroalkylsulfonate anions ($C_nF_{2n+1}SO_3^-$, n = 1, 4, and 8) and perfluoroalkylcarboxylate anions ($C_nF_{2n+1}CO_2^-$, n = 1–4) have been prepared. CF_3SO_3 is abbreviated to OTf. For comparison, we have also prepared cobaltocenium salts and octamethylferrocenium salts with these anions. All the salts investigated in this study were found to exhibit phase transitions in the solid state. These salts were crystallographically examined to elucidate the characteristics of the perfluoroalkyl chains in the solid state.

2. Results and discussion

2.1. Preparation and thermal properties

The salts with OTf^- or $C_nF_{2n+1}CO_2^-$ (n = 1–4) were prepared by chemical oxidation of metallocenes with silver salts of the corresponding anions. The salts with $C_nF_{2n+1}SO_3^-$ (n = 4 or 8) were prepared by anion exchange of metallocenium nitrates. $[FeCp^*_2](CF_3CO_2)\cdot 1/3H_2O$ and $[FeCp^*_2](C_2F_5CO_2)\cdot H_2O$ were obtained as hydrates.

The melting points and decomposition temperatures of these salts are listed in Table 1. The decomposition temperatures of the sulfonate salts were 312–348 °C, determined by thermogravimetric (TG) analysis (−3 wt%). The OTf salts decomposed without melting, whereas $[FeCp^*_2](C_4F_9SO_3)$ and $[CoCp^*_2](C_4F_9SO_3)$ melted at around 250 °C, and $[FeCp^*_2](C_8F_{17}SO_3)$ melted at 287 °C, before decomposition. In contrast, the carboxylate salts were much less thermally stable; $[FeCp^*_2](C_nF_{2n+1}CO_2)$ (n = 1–4) and the corresponding octamethylferrocenium salts decomposed at temperatures below 180 °C without melting, as a result of thermal decomposition of the anions [9].

Dehydration of the hydrate salts was observed by TG analysis. In $[FeCp^*_2](CF_3CO_2)\cdot 1/3H_2O$, a slight weight loss corresponding to dehydration occurred at around 104 °C (−1.3 wt%), although this was not clear, and decomposition occurred at 125 °C (−3 wt%). $[FeCp^*_2](C_2F_5CO_2)\cdot H_2O$ exhibited a weight loss of −3.2% at 105 °C, which corresponds to dehydration (calcd −3.5 wt%), and decomposition started at 153 °C (−3 wt%).

2.2. Phase transitions in the solid state

All the salts exhibited phase transitions in the solid state. Thermal data for the phase transitions, determined by differential scanning calorimetry (DSC) measurements, are listed in Tables 2–4.

The phase sequences of the sulfonate salts $[MCp^*_2](C_nF_{2n+1}SO_3)$ (M = Fe and Co) are shown schematically in Fig. 1. The transition temperatures and transition entropies are shown in the figure. In these salts, differences in metal species were found to affect the phase behaviors, as reported for $[MCp_2][PF_6]$ [10]. $[FeCp^*_2](OTf)$, which exhibited phase transitions at −120.6 °C (ΔS = 4.9 J mol^{-1} K^{-1}) and 146.5 °C (ΔS = 31.4 J mol^{-1} K^{-1}); the latter is probably a transition to a plastic phase. Despite being isostructural at room temperature (vide infra), $[CoCp^*_2](OTf)$ exhibited no phase transitions at low temperatures, whereas the salt exhibited a broad, successive transition at around 112.7 °C (ΔS =

25.2 J mol^{-1} K^{-1}). In $[MCp^*_2](C_4F_9SO_3)$ (M = Fe, Co), the ferrocenium salt exhibited complicated phase behavior, showing phase transitions at −37.4 °C, −0.6 °C, and 88.6 °C (sum of the transition entropies: ΔS_{total} = 16.6 J mol^{-1} K^{-1}), whereas the cobaltocenium salt exhibited only one phase transition with a small transition entropy (< 2 J mol^{-1} K^{-1}) at −111.9 °C. $[FeCp^*_2](C_8F_{17}SO_3)$ exhibited only one phase transition with a small transition entropy at −30.5 °C.

The phase sequences of the carboxylate salts $[FeCp^*_2](C_nF_{2n+1}CO_2)$ (n = 1–4) are shown in Fig. 2a. $[FeCp^*_2](CF_3CO_2)\cdot H_2O$ exhibited three phase transitions, at −5.3 °C, 57.0 °C, and 72.0 °C (ΔS_{total} = 58.2 mol^{-1} K^{-1}). The salt with n = 2 exhibited a transition at 64.4 °C (ΔS = 79.1 J mol^{-1} K^{-1}). The large transition entropies indicate that their high-temperature phases are highly disordered. In contrast, the salts with n = 3 and 4 exhibited transitions with small transition entropies at −114.7 °C and −114.3 °C, respectively.

The phase sequences of the corresponding octamethylferrocenium salts (n = 1–3) are shown in Fig. 2b. The salt with n = 1 exhibited a solid-phase transition at 35.6 °C (ΔS = 22.0 J mol^{-1} K^{-1}). The salt with n = 2 exhibited two phase transitions at 24.2 °C and 39.6 °C with small transition entropies. The salts with n = 3 exhibited three phase transitions at −35.4 °C, 14.7 °C, and 41.5 °C (ΔS_{total} = 25.3 J mol^{-1} K^{-1}). Although it is not possible to simply compare these data with those for decamethylferrocenium, because of their different compositions, it is likely that the octamethylferrocenium salts exhibit more phase transitions, as seen by comparison with the salts with $C_3F_7CO_2^-$. Some of these phase transitions may be related to the order–disorder transitions of octamethylferrocene [7].

The results of the calorimetric analyses suggest that salts with longer perfluoroalkyl chains in the anion tend to exhibit simpler phase sequences and smaller entropies of solid-phase transitions. Since the melting entropies of these salts could not be measured because of their high melting points or decomposition, no discussion of the residual entropies at low temperatures is possible. However, it is highly plausible that disorder of the perfluoroalkyl chains remains at low temperatures for anions with longer chains, as is also suggested crystallographically (vide infra).

2.3. Structural changes in [FeCp$_2$](OTf) associated with phase transition*

[FeCp*$_2$](OTf) exhibited a phase transition at −121.6 °C. We performed X-ray analyses of this salt above and below the phase-transition temperature. The crystallographic parameters determined at −100 °C and −153 °C are listed in Table 5. The packing diagram for the room-temperature phase at −100 °C is shown in Fig. 3a. The crystal belongs to the orthorhombic system with space group *P*mn2$_1$, which is a polar space group. In the unit cell, one cation is surrounded by eight anions, and vice versa, showing a cesium-chloride-like cation–anion arrangement. The C_5-axis of the cation and the C_3-axis of the anion are arranged parallel along the [01−1] direction. The space group imposes C_σ symmetry on both the cation and the anion. The OTf anions are ordered. In the cation, one of the Cp* rings exhibits elongated thermal ellipsoids, which suggests the presence of disorder [7]. This is presumably ascribable to steric effects between the cation and anion; the Cp* ring adjacent to the trifluoromethyl groups has more room, which allows disorder, whereas the larger sulfonate group sterically hinders the motion of the neighboring Cp* ring. In the *bc*-plane, the orientations of the cations and anions are aligned in one direction (Fig. 3). The molecular orientations in the neighboring planes are almost perpendicular. However, the polarity remains along the *c* direction, and this results in a polar space group.

The structure of the low-temperature phase is shown in Fig. 3b. The space group changed to *P*1, and a superstructure was formed. The repeating units became three times and two times longer with respect to the *a*- and *b*-axes, respectively, compared with the room-temperature structure (Fig. 3b, dashed lines). The unit cell contains 12 cations and anions. The Cp* rings in the cation are ordered, and the unit cell contains eight cations with the eclipsed conformation and four cations with the staggered conformation, indicated by (E) and (S), respectively, in Fig. 3b. The superstructure originates from the different conformers of the cations and canting of the OTf anions. The conformational differences among the cations as well as the polar orientation of the anion resulted in a non-centrosymmetric space group.

In contrast to [FeCp*$_2$](OTf), no phase transition was observed in [CoCp*$_2$](OTf) at low temperatures. The crystal structure of this salt at −183 °C was found to be isomorphous (orthorhombic *P*mn2$_1$) with the room-temperature phase of [FeCp*$_2$](OTf), with cell parameters a = 12.471(2) Å, b =

8.709(1) Å, c = 9.692(2) Å, and V = 1069.6(3) Å. The cell volume of the cobaltocenium salt was slightly smaller than that of the ferrocenium salt, which is consistent with the smaller molecular volume of the cobaltocenium cation.

2.4. Structural changes in [FeCp$_2$](C$_3$F$_7$CO$_2$) associated with phase transition*

[FeCp*$_2$](C$_3$F$_7$CO$_2$) exhibited a phase transition at −115 °C. The crystallographic parameters of this salt determined at −173 °C and at −100 °C are listed in Table 6. The packing diagrams in the high-temperature phase and in the low-temperature phase are shown in Figs. 4a and b, respectively. The space group ($P2_1/c$) was unchanged, and the unit-cell parameters as well as the molecular arrangement were nearly the same in both phases. The thermal ellipsoids of the anion are very large in the high-temperature phase, suggesting molecular libration or displacements, whereas they are suppressed in the low-temperature phase. The cations and anions are slightly rotated, approximately around the [104] direction associated with the phase transition. The anions may attain larger space for librations in the high-temperature phase as a result of rearrangement of the molecular packing. In the unit cell, the fluoroalkyl groups of the anions are in contact with each other along the *b*-axis, whereas the carboxylate groups are surrounded by cations. One of the Cp* rings of the cation faces the fluoroalkyl moiety of the anion, and the other ring is close to the Cp* ring of an adjacent cation.

2.5. Crystallographic features of other salts

The unit-cell parameters for [FeCp*$_2$](C$_n$F$_{2n+1}$SO$_3$) (n = 4 and 8) and [FeCp*$_2$](C$_4$F$_9$CO$_2$) determined at −173 °C are listed in Table 7. In these salts, the structures could not be fully refined because of the extensive disorder of the perfluoroalkyl chains. The structures of [MCp*$_2$](C$_4$F$_9$SO$_3$) (M = Fe and Co) are different from each other, and this is probably associated with their different phase sequences. A Cambridge Structural Database (CSD) search revealed that the structures of about a dozen compounds involving perfluoroalkylsulfonate or perfluoroalkylcarboxylate anions with $n > 2$ are known. They are mostly disordered [11], and there are fewer known structures of perfluoroalkylsulfonates than of perfluoroalkylcarboxylates. This may be partly ascribed to the difficulty of analyzing the structures of such compounds, which are often accompanied by extensive

disorder, as seen in the present study.

2.6. Solid-state ^{13}C NMR

Solid-state ^{13}C NMR spectra of $[MCp^*_2](C_4F_9SO_3)$ (M = Fe, Co) were investigated. In the magic-angle-spinning (MAS) NMR spectrum of $[FeCp^*_2](C_4F_9SO_3)$ (Fig. 5a), peaks of the ring and methyl carbons were observed at 253 ppm and –24 ppm, respectively, as broad peaks resulting from paramagnetism of the cation. The chemical shifts are in accordance with the literature values for decamethylferrocenium salts [12]. The fluoroalkyl carbons of the anion were observed at around 115 ppm, which is the usual chemical shift for fluoroalkanes [13]. The broadness of the peak is ascribed to dipole–dipole interactions with the fluorine atoms. A MAS NMR spectrum of the diamagnetic salt $[CoCp^*_2](C_4F_9SO_3)$ (Fig. 5b) exhibited sharp peaks corresponding to the ring and methyl carbons at 94.6 ppm and 8.3 ppm, respectively. The fluoroalkyl carbons were observed at 112 ppm as a broad peak because of the dipole–dipole interactions. To detect possible changes in molecular motion at low temperatures, the temperature dependence of static NMR spectra were also measured for this salt, but the spectra were unchanged in the temperature range down to −93 °C.

3. Conclusion

Decamethylferrocenium salts with perfluoroalkylsulfonate and perfluoroalkylcarboxylate anions were prepared and their thermal behaviors characterized. The carboxylate salts were thermally less stable than the sulfonates. These salts exhibited phase transitions in the solid state, and the corresponding decamethylcobaltocenium salts exhibited different phase sequences. Crystallographic investigations revealed structural changes associated with the phase transitions in two salts. In $[Fe(C_5Me_5)_2](CF_3SO_3)$, the transition is associated with the ordering of the cation conformations into eclipsed and staggered conformations in different ratios at low temperatures. The unit-cell volume became six times larger as a result of this ordering. The phase transitions in $[Fe(C_5Me_5)_2](C_3F_7CO_2)$ at low temperatures were accompanied by suppression of libration or displacements of the anion, associated with rotational rearrangements of molecules in the unit cell. The phase transitions in other salts are probably associated with order–disorder transitions, as a result of the nearly spherical

molecular shapes of the cations and the characteristics of the fluorinated anions. A general tendency of the perfluoroalkyl anions to give extensive disorder even at low temperatures was found. Investigation of the thermal properties of alkylferrocenium salts with lower melting points is underway in our laboratories.

4. Experimental

4.1. General

[FeCp*$_2$], [CoCp*$_2$], $LiCF_3CO_2$, AgOTf, and $AgC_nF_{2n+1}CO_2$ (n = 1–3) were purchased from Sigma-Aldrich. $C_4F_9CO_2H$, $AgNO_3$, and $LiC_nF_{2n+1}SO_3$ (n = 4 and 8) were purchased from Wako. $AgC_4F_9CO_2$ was prepared according to a literature method [14]. Elemental analyses were carried out using a Yanaco MT5 analyzer. DSC measurements were performed using a TA Instrument Q100 differential scanning calorimeter in the temperature range 90–430 K at a scan rate of 10 K min^{-1}. Thermogravimetric (TG) analyses were performed on a Rigaku TG8120 under a nitrogen atmosphere at a heating rate of 5 K min^{-1}. Solid-state NMR spectra were recorded on a Tecmag Apollo spectrometer (operating at 75.431 MHz for ^{13}C and 299.9515 MHz for ^{1}H) equipped with a Doty XC MAS 4-mm probe head in the temperature range 180–298 K.

4.2. [MCp$_2$](NO$_3$) (M = Fe, Co)*

To a stirred solution of [FeCp*$_2$] (200 mg, 0.612 mmol) in acetone was added an aqueous solution of a slight excess of $AgNO_3$ (120 mg, 0.706 mmol). The mixture was stirred for 30 min, and the solution was filtered to remove silver deposits and excess silver salt. After evaporation of the solvent, the residue was extracted with dichloromethane (100 mL) and washed with water. The organic phase was dried over magnesium sulfate and evaporated to give green crystals of [FeCp*$_2$](NO_3) in 84% yield. FT–IR (KBr, cm^{-1}): 1020, 1370 (NO), 1620, 1745, 2955. [CoCp*$_2$](NO_3) was prepared similarly, under a nitrogen atmosphere, using decamethylcobaltocene (39.5 mg, 0.120 mmol) and silver nitrate (19 mg, 0.112 mmol), yielding 34.1 mg of yellow crystals in 80% yield. FT-IR (KBr, cm^{-1}): 1025, 1352 (NO), 1629, 1680. These salts were used for anion-exchange reactions without further purification

4.3. [MCp$_2$](OTf) (M = Fe, Co)*

AgOTf (13.8 mg, 5.37 × 10^{-2} mmol) in acetonitrile was added dropwise to an acetonitrile solution of [FeCp*$_2$] (15.8 mg, 4.84 × 10^{-2} mmol). After stirring for 1 h at room temperature, the solution was filtered, evaporated, and the residue was dried under vacuum. The powder was again dissolved in acetonitrile, filtered, evaporated, and dried under vacuum to produce 21 mg of [FeCp*$_2$](OTf) (91% yield). The product was recrystallized by slow diffusion of diethyl ether into an acetonitrile solution. Anal. Calcd (%) for $C_{11}H_{10}F_3FeO_3S$: C, 53.05; H, 6.37; N, 0. Found C, 53.26; H, 6.57; N, 0. FT–IR (cm^{-1}): 748, 1026, 1134 (SO), 1274 (SO), 1384, 1479. [CoCp*$_2$](OTf) was prepared by the same method, using AgOTf (36.0 mg, 0.14 mmol), [CoCp*$_2$] (49.4 mg, 0.15 mmol), and acetone solvent, under a nitrogen atmosphere. Yellow plate crystals were obtained in 89% yield. Anal. Calcd (%) for $C_{21}H_{30}F_3O_3SCo$: C, 52.72; H, 6.32; N, 0. Found: C, 52.36; H, 6.32; N, 0. FT–IR (cm^{-1}): 748, 1026, 1149 (SO), 1280 (SO), 1384, 1483.

4.4. [MCp$_2$]($C_nF_{2n+1}SO_3$) (n = 4 and 8; M = Fe, Co)*

Water solutions of [FeCp*$_2$](NO_3) (50 mg, 0.111 mmol) and $LiC_4F_9SO_3$ (43.5 mg, 0.142 mmol) were mixed and stirred for 30 min, and then extracted with dichloromethane. The organic phase was washed with water, dried over magnesium sulfate, and evaporated, to produce 64.1 mg of [FeCp*$_2$]($C_4F_9SO_3$) (47% yield). The product was recrystallized from dichloromethane–hexane. Calcd (%) for $C_{24}H_{30}O_3SFeF_9$: C, 46.09; H, 4.84; N, 0. Found: C, 46.07; H, 5.01; N, 0. FT–IR (cm^{-1}): 652, 667, 1128 (SO), 1228, 1261 (SO). [CoCp*$_2$]($C_4F_9SO_3$) was prepared by the same method, using [CoCp*$_2$](NO_3) (50 mg, 0.111 mmol) and $LiC_4F_9SO_3$ (47.3 mg, 0.154 mmol), to produce 59.0 mg of the product (85% yield). The product was recrystallized by slow diffusion of diethyl ether into a dichloromethane solution. Calcd (%) for $C_{24}H_{30}O_3SCoF_9$: C, 45.87; H, 4.81; N, 0. Found: C, 45.63; H, 4.83; N, 0. FT–IR (cm^{-1}): 653, 1052, 1129 (SO), 1207, 1264 (SO), 1482. [FeCp*$_2$]($C_8F_{17}SO_3$) was obtained by the same procedure, in 54% yield. When extracting this salt, a saturated aqueous solution of sodium chloride was added. Calcd (%) for $C_{28}H_{30}O_3SFeF_{17}$: C, 40.74; H, 3.66; N, 0. Found: C, 40.56; H, 3.70; N, 0. FT–IR (cm^{-1}): 618, 751, 1030, 1144 (SO), 1195, 1261 (SO).

4.5. [FeCp$_2$]($C_nF_{2n+1}CO_2$) (n = 1–4)*

A water solution of $AgCF_3CO_2$ (37.1 mg, 0.168 mmol) was added dropwise to an acetone solution of [FeCp*$_2$] (50 mg, 0.153 mmol). After stirring the solution for 30 min, silver deposits were removed by filtration, and the filtrate was evaporated, and extracted with dichloromethane. The organic layer was dried over magnesium sulfate to produce 59 mg of [FeCp*$_2$](CF_3CO_2) (88% yield). The product was recrystallized from a mixture of dichloromethane and diethyl ether. [FeCp*$_2$](CF_3CO_2)·1/3 H_2O: Calcd (%) for $C_{22}H_{30.66}O_{2.33}FeF_3$: C, 59.34; H, 6.94; N, 0. Found: C, 59.22; H, 7.19; N, 0. FT–IR (KBr, cm^{-1}): 785, 834, 987, 1050, 1309, 1497, 1679 (CO), 2350. Other salts were prepared similarly. [FeCp*$_2$]($C_2F_5CO_2$)·H_2O: 78% yield. Calcd (%) for $C_{23}H_{32}O_3FeF_5$: C, 54.45; H, 6.36; N, 0. Found: C, 54.79; H, 6.35; N, 0. FT–IR (KBr, cm^{-1}): 783, 821, 1050, 1212, 1232, 1322, 1370, 1460, 1681 (CO) 2371. [FeCp*$_2$]($C_3F_7CO_2$): 60% yield. Calcd (%) for $C_{24}H_{30}O_2FeF_7$: C, 53.45; H, 5.61; N, 0. Found: C, 53.36; H, 5.68; N, 0.18. FT–IR (cm^{-1}): 763, 792, 811, 957, 982, 1108, 1220, 1324, 1697 (CO), 2360. [FeCp*$_2$]($C_4F_9CO_2$): 71.2% yield. Calcd (%) for $C_{25}H_{30}O_2FeF_9$: C, 50.95; H, 5.13; N, 0. Found: C, 51.30; H, 5.54; N, 0. FT–IR (cm^{-1}): 711, 737, 793, 953, 1023, 1107, 1191, 1219, 1323, 1695 (CO), 2916.

4.6. [Fe(C_5Me_4H)$_2$]($C_nF_{2n+1}CO_2$) (n = 1–3)

These salts were prepared as described for [FeCp*$_2$]($C_nF_{2n+1}CO_2$). The products were recrystallized from mixtures of dichloromethane and hexane. [Fe(C_5Me_4H)$_2$](CF_3CO_2): 86% yield. Calcd (%) for $C_{20}H_{26}O_2FeF_3$: C, 58.41; H, 6.37; N, 0. Found: C, 58.72; H, 6.48; N, 0. FT–IR (cm^{-1}): 668, 813, 1025, 1196, 1691 (CO), 2020, 2359. [Fe(C_5Me_4H)$_2$]($C_2F_5CO_2$): 96% yield. Calcd (%) for $C_{21}H_{26}O_2FeF_5$: C, 54.68; H, 5.68; N, 0. Found: C, 54.75; H, 5.78; N, 0. FT–IR (KBr, cm^{-1}): 692, 781, 1169, 1201, 1680 (CO), 2350. [Fe(C_5Me_4H)$_2$]($C_3F_7CO_2$): 98% yield. Calcd (%) for $C_{22}H_{36}O_2FeF_7$: C, 50.68; H, 6.96; N, 0. Found: C, 50.48; H, 6.56; N, 0. FT–IR (cm^{-1}): 725, 765, 1011, 1148, 1200, 1309, 1692 (CO), 2360.

4.7. X-ray crystallography

X-ray diffraction data for single crystals of [FeCp*$_2$](OTf), [CoCp*$_2$](OTf), and

[$FeCp^*_2$]($C_3F_7CO_2$) were collected on a Bruker SMART APEX II CCD diffractometer, using Mo Kα radiation (λ = 0.71073 Å). Crystal data, data collection parameters, and analysis statistics for these compounds are listed in Tables 5 and 6. The data were corrected for absorption using the SADABS program [15]. All calculations were performed using SHELXL [16]. The structure was solved by direct methods (SHELXS 97) and expanded using Fourier techniques. The non-hydrogen atoms were refined anisotropically. Empirical absorption corrections were applied. The hydrogen atoms were inserted at the calculated positions and allowed to ride on their respective parent atoms. ORTEP-3 [17] was used for molecular graphics. Although the unit cell of [$FeCp^*_2$](OTf) in the low-temperature phase was very close to orthorhombic, the correct space group turned out to be triclinic *P*1. Although a check using the PLATON program [18] suggests *P*mn2_1, this space group is improbable because different conformers overlap and disorder is caused by symmetry constraints. Analyses assuming the monoclinic space groups *P*2_1, *P*n, and *P*c also resulted in improbable disordered structures.

CCDC-822999 ([$FeCp^*_2$](OTf) at −100 °C), CCDC-823000 ([$FeCp^*_2$](OTf) at −153 °C), CCDC-823460 ([$FeCp^*_2$]($C_3F_7CO_2$) at −100 °C), and CCDC-790933 ([$FeCp^*_2$]($C_3F_7CO_2$) at −173 °C) contain the supplementary crystallographic data for this paper. These data can be obtained free of charge from the Cambridge Crystallographic Data Centre via www.ccdc.cam.ac.uk/data_request/cif. Diffraction data for the other salts were collected at −173 °C, but their structures could not be fully determined because of extensive disorder, and only cell parameters are listed in Table 7.

Acknowledgements

We thank Y. Furuie (Kobe University) for elemental analyse and M. Nakama (Crayonsoft Inc., Tokyo) for providing a Web-DB system. This work was financially supported by KAKENHI (No. 21350077) from the Japan Society for the Promotion of Science (JSPS). We also thank the anonymous reviewers for their valuable comments.

Appendix. Supplementary material

Supplementary data related to this article can be found online at doi:10.1016/j.jorganchem. Crystallographic CIF file for [$FeCp^*_2$](OTf) and [$FeCp^*_2$]($C_3F_7CO_2$).

References

[1] (a) D. Braga, F. Grepioni, Chem. Soc. Rev. 29 (2000) 229–238;

(b) D. Braga,. F. Grepioni, Topics in Organometallic Chemistry, in: J.M. Brown, P. Hofmann (Eds.), Springer, Berlin, Heidelberg, 1999, pp. 47−68;

(c) D. Braga, M. Curzi, S. L. Giaffreda, F. Grepioni, L. Maini, A. Pettersen, M. Polito, Chap. 12, in "Ferrocenes: Ligands, Materials and Biomolecules, ed. P. Štěpnička, John Wiley & Sons Ltd, Chichester (2008).

[2] R.J. Webb, M.D. Lowery, Y. Shiomi, M. Sorai, R.J. Wittebort, D.N. Hendrickson, Inorg. Chem. 31 (1992) 5211–5219.

[3] (a) H. Schottenberger, K. Wurst, U.J. Griesser, R.K.R. Jetti, G. Laus, R.H. Herber, I. Nowik, J. Am. Chem. Soc. 127 (2005) 6795–6801;

(b) I. Nowik, R.H. Herber, Inorg. Chim. Acta 310 (2000) 191–195.

[4] D. Braga, L. Scaccianoce, F. Grepioni, S.M. Draper, Organometallics 15 (1996) 4675–4677.

[5] (a) T. Mochida, K. Takazawa, M. Takahashi, M. Takeda, Y. Nishio, M. Sato, K. Kajita, H. Mori, M.M. Matsusita, T. Sugawara, J. Phys. Soc. Jpn. 74 (2005) 2214–2216;

(b) T. Mochida, K. Takazawa, H. Matsui, M. Takahashi, M. Takeda, M. Sato, Y. Nishio, K. Kajita, H. Mori, Inorg. Chem. 44 (2005) 8628–8641.

[6] (a) T. Mochida, K. Yoza, J. Organomet. Chem. 695 (2010) 1749–1752;

(b) T. Mochida, Y. Funasako, H. Azumi, Dalton Trans. 40 (2011) 9221–9228;

(c) Y. Funasako, T. Mochida, Kenji Yoza, J. Organomet. Chem. 698 (2012) 49–52.

[7] (a) T. Inagaki, T. Mochida, Chem. Lett. 39 (2010) 572–573;

(b) T. Inagaki, T. Mochida, M. Takahashi, C. Kanadani, T. Saito, D. Kuwahara, Chem. Eur. J. doi: 10.1002/chem.201200151;

(c) Y. Funasako, T. Mochida, T. Inagaki, T. Sakurai, H. Ohta, K. Furukawa, T. Nakamura, Chem. Commun. 47 (2011) 4475–4477.

[8] (a) M. Armand, F. Endres, D.R. MacFarlane, H. Ohno, B. Scrosati, Nature Mater. 8 (2009) 621–629;

(b) I. Krossing, J.M. Slattery, C. Daguenet, P.J. Dyson, A. Oleinikova, H. Weingärtner, J. Am. Chem. Soc. 128 (2006) 13427–13434.

[9] P. Bonhôte, A. Dias, N. Papageorgiou, K. Kalyanasundaram, M. Grätzel, Inorg. Chem. 35 (1996) 1168–1178.

[10] F. Grepioni, G. Cojazzi, S.M. Draper, N. Scully, D. Braga, Organometallics 17 (1998) 296–307.

[11] S. Rau, L. Böttcher, S. Schebesta, M. Stollenz, H. Görls, D. Walther, Eur. J. Inorg. Chem. 11 (2002) 2800–2809.

[12] H. Heise, F.H. Köhler, M. Herker, W. Hiller, J. Am. Chem. Soc. 124 (2002) 10823–10832.

[13] S.K. Quek, I.M. Lyapkalo, H.V. Huynh, Tetrahedron 62 (2006) 3137–3145.

[14] M. Hausptschein, A.V. Grosse, J. Am. Chem. Soc. 73 (1951) 2461–2463.

[15] G.M. Sheldrick, SADABS: Program for Semi-empirical Absorption Correction, University of Göttingen, Germany (1997).

[16] G.M. Sheldrick, Program for the Solution for Crystal Structures, University of Göttingen, Germany (1997).

[17] L.J. Farrugia, J. Appl. Cryst. 30 (1997) 565.

[18] A.L. Spec, PLATON – A Multipurpose Crystallographic Tool, Utrecht University, The Netherlands (2011).

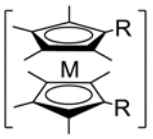

$X = C_nF_{2n+1}SO_3^-$

M	R	X
Fe	Me	OTf^-
Co	Me	OTf^-
Fe	Me	$C_4F_9SO_3^-$
Co	Me	$C_4F_9SO_3^-$
Fe	Me	$C_8F_{17}SO_3^-$

$X = C_nF_{2n+1}CO_2^-$

M	R	X
Fe	Me	$CF_3CO_2^-$
Fe	Me	$C_2F_5CO_2^-$
Fe	Me	$C_3F_7CO_2^-$
Fe	Me	$C_4F_9CO_2^-$
Fe	H	$CF_3CO_2^-$
Fe	H	$C_2F_5CO_2^-$
Fe	H	$C_3F_7CO_2^-$

Chart 1. Chemical formulas of metallocenium salts with perfluoroalkyl-sulfonate and -carboxylate anions.

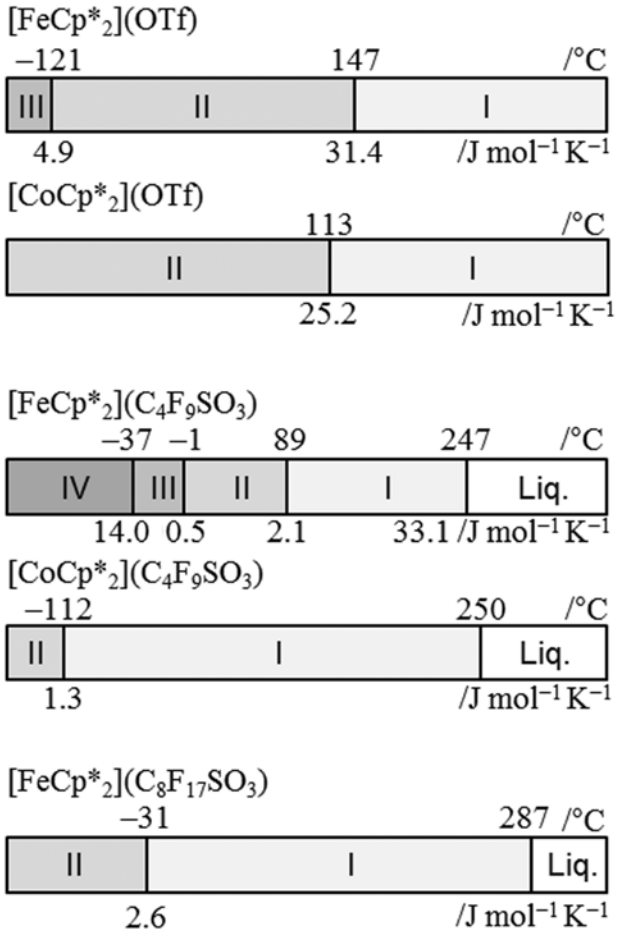

Fig. 1. Phase sequences of $[MCp^*_2](C_nF_{2n+1}SO_3)$ (M = Fe, Co). The phase- transition temperatures (°C) and transition entropies (J mol^{-1} K^{-1}) are shown above and below each diagram, respectively.

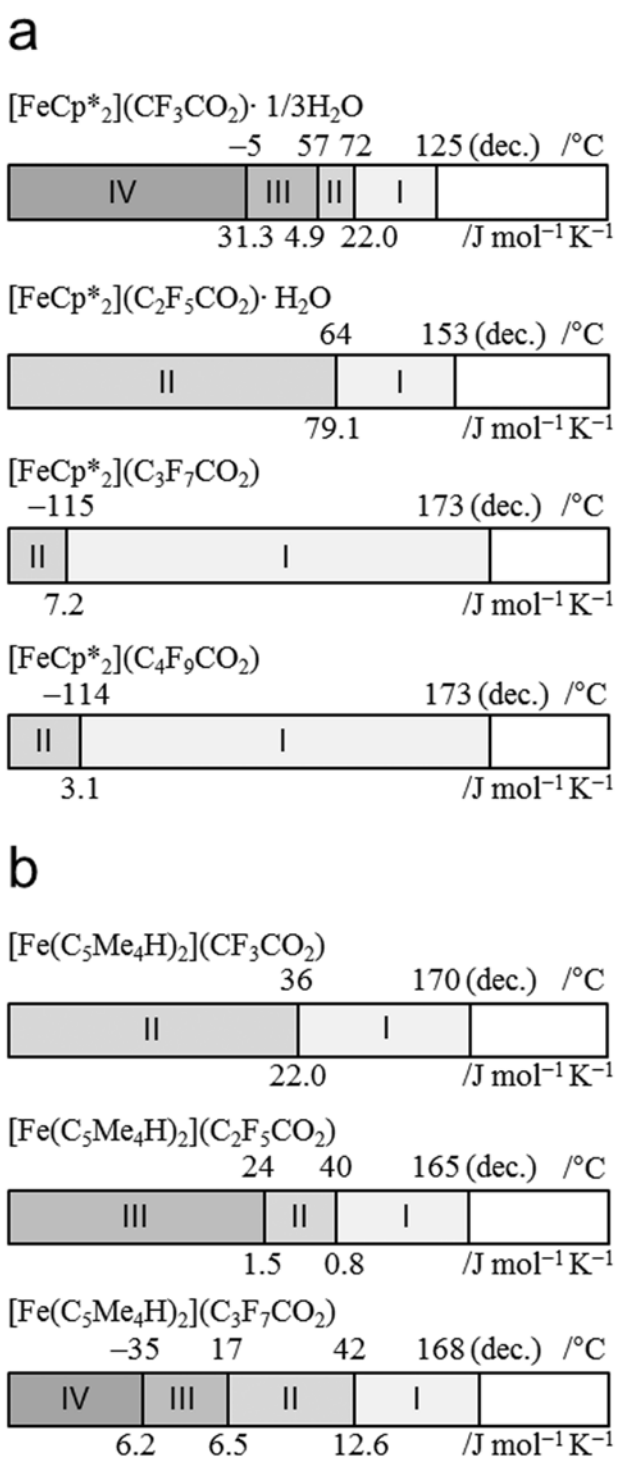

Fig. 2. Phase sequences of (a) $[FeCp^*_2](C_nF_{2n+1}CO_2)$ and (b) $[Fe(C_5Me_4H)_2](C_nF_{2n+1}CO_2)$. The phase-transition temperatures (°C) and transition entropies (J mol^{-1} K^{-1}) are shown above and below each diagram, respectively.

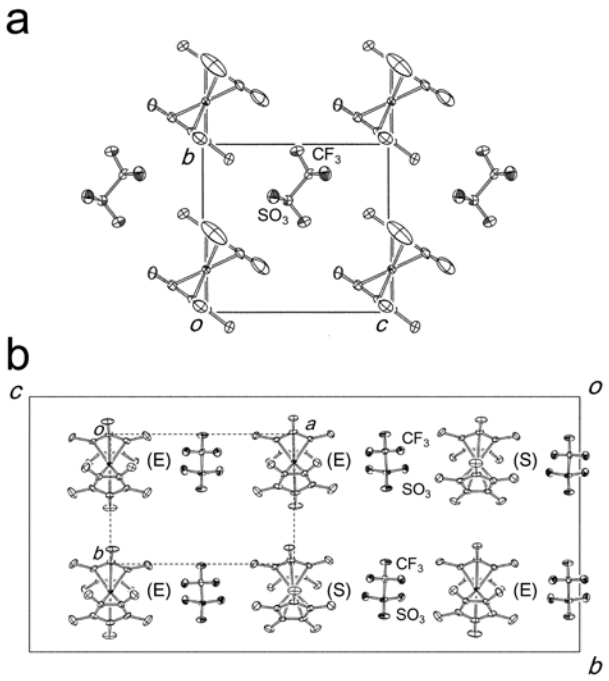

Fig. 3. Packing diagrams of [FeCp*$_2$](OTf) determined at (a) –100 °C (room-temperature phase) and (b) –153 °C (low-temperature phase). Only half of the unit-cell contents are shown for clarity. In the low-temperature structure, the corresponding room-temperature unit cell is shown by dashed lines, and the conformations of the cation are indicated by E (eclipsed) and S (staggered). Hydrogen atoms have been omitted for clarity.

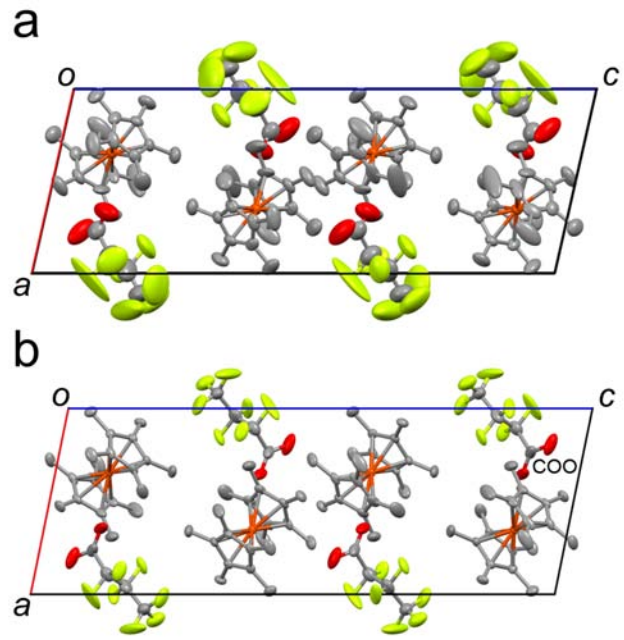

Fig. 4. Packing diagram of [FeCp*$_2$]($C_3F_7CO_2$) determined at (a) –100 °C (room-temperature phase) and (b) –173 °C (low-temperature phase). Hydrogen atoms have been omitted for clarity.

Table 1

Melting points (T_m) and decomposition temperatures (T_{dec}) of metallocenium salts with perfluoroalkyl-sulfonate and -carboxylate anions.

Compounds	T_m	T_{dec}
$[FeCp^*_2](OTf)$	–[a]	316[b]
$[CoCp^*_2](OTf)$	–[a]	322[b]
$[FeCp^*_2](C_4F_9SO_3)$	249	323[b]
$[CoCp^*_2](C_4F_9SO_3)$	250	348[b]
$[FeCp^*_2](C_8F_{17}SO_3)$	287	312[b]
$[FeCp^*_2](CF_3CO_2)\cdot$ 1/3 H_2O	–[a]	104[b,d], 125[b]
$[FeCp^*_2](C_2F_5CO_2)\cdot H_2O$	–[a]	105[b,d], 153[b]
$[FeCp^*_2](C_3F_7CO_2)$	–[a]	173[b]
$[FeCp^*_2](C_4F_9CO_2)$	–[a]	173[c]
$[Fe(C_5Me_4H)_2](CF_3CO_2)$	–[a]	170[b]
$[Fe(C_5Me_4H)_2](C_2F_5CO_2)$	–[a]	165[b]
$[Fe(C_5Me_4H)_2](C_3F_7CO_2)$	–[a]	168[b]

[a] Decomposed before melting.

[b] Determined by TG analysis (–3 wt%).

[c] Visually determined.

[d] Dehydration.

Table 2

Thermal data for the phase transitions in $[MCp^*_2](C_nF_{2n+1}SO_3)$.

Compound	Phase transitions	T (°C)	ΔH (kJ mol^{-1})	ΔS (J mol^{-1} K^{-1})	ΔT (°C)
$[FeCp^*_2](OTf)$	III → II	–120.6	0.7	4.9	0.9
	II → I	146.5	13.2	31.4	10.4
$[CoCp^*_2](OTf)$	II → I	112.7	9.7	25.2	1.5
$[FeCp^*_2](C_4F_9SO_3)$	IV → III	–37.4	3.3	14.0	8.9
	III → II	–0.6	0.1	0.5	1.4
	II → I	88.6	0.8	2.1	2.1
	I → Liquid	248.8	17.2	33.1	12.1
$[CoCp^*_2](C_4F_9SO_3)$	II → I	–111.9	0.2	1.3	10.5
$[FeCp^*_2](C_8F_{17}SO_3)$	II → I	–30.5	0.6	2.6	2.7

Table 3

Thermal data for the phase transitions in $[MCp^*_2](C_nF_{2n+1}CO_2)$.

Compound	Phase transitions	T (°C)	ΔH (kJ mol^{-1})	ΔS (J mol^{-1} K^{-1})	ΔT (°C)
$[FeCp^*_2](CF_3CO_2)\cdot$ 1/3 H_2O	IV → III	–5.3	8.4	31.3	13.1
	III → II	57.0	1.6	4.9	16.6
	II → I	72.0	7.6	22.0	6.8
$[FeCp^*_2](C_2F_5CO_2)\cdot H_2O$	II → I	64.4	26.7	79.1	5.5
$[FeCp^*_2](C_3F_7CO_2)$	II → I	–114.7	1.1	7.2	3.3
$[FeCp^*_2](C_4F_9CO_2)$	II → I	–114.3	0.5	3.1	3.5

Table 4

Thermal data for the phase transitions in $[Fe(C_5Me_4H)_2](C_nF_{2n+1}CO_2)$.

Compound	Phase transitions	T (°C)	ΔH (kJ mol^{-1})	ΔS (J mol^{-1} K^{-1})	ΔT (°C)
$[Fe(C_5Me_4H)_2](CF_3CO_2)$	II → I	35.6	6.1	22.0	9.9
$[Fe(C_5Me_4H)_2](C_2F_5CO_2)$	III → II	24.2	0.5	1.5	12.3
	II → I	39.6	0.3	0.8	10.3
$[Fe(C_5Me_4H)_2](C_3F_7CO_2)$	IV → III	–35.4	4.5	6.2	36.1
	III → II	14.7	5.7	6.5	15.3
	II → I	41.5	11.9	12.6	11.7

[a] Determined by TG analysis.

Table 5

Crystallographic parameters for [FeCp*$_2$](OTf) at 120 K and 173 K.

	120 K	173 K
Empirical formula	$C_{21}H_{30}F_3FeO_3S$	
Formula weight (g mol^{-1})	475.36	
Temperature (K)	120	173
Crystal system	Triclinic	Orthorhombic
Space group	$P1$	$Pmn2_1$
Crystal size (mm^3)	0.71×0.59×0.47	0.20×0.15×0.10
a (Å)	9.6832(13)	12.693(3)
b (Å)	17.587(2)	8.783(2)
c (Å)	37.869(5)	9.715(2)
α (°)	89.964(2)	90
β (°)	89.964(2)	90
γ (°)	89.960(2)	90
Volume (Å^3)	6449.1(15)	1083.1(4)
Z	12	2
$d_{calcd.}$ (g cm^{-3})	1.469	1.458
Reflections collected	36265	7840
Independent reflections	31163	2700
Parameters	3134	146
R_1[a], wR_2[b] ($I > 2\sigma(I)$)	0.0396, 0.1059	0.0562, 0.1364
R_1[a], wR_2[b] (all data)	0.0586, 0.1174	0.0888, 0.1557
Goodness-of-fit on F^2	1.075	1.008

[a] $R_1 = \Sigma \, ||F_o| - |F_c|| \, / \, \Sigma \, |F_o|$.

[b] $wR_2 = [\, \Sigma \, w(F_o^2 - F_c^2)^2 \, / \, \Sigma \, w(F_o^2)^2 \,]^{1/2}$.

Table 6

Crystallographic parameters for $[FeCp^*_2](C_3F_7CO_2)$ at 100 K and 173 K.

	100 K	173 K
Empirical formula	$C_{24}H_{30}F_7FeO_2$	
Formula weight (g mol^{-1})	539.33	
Temperature (K)	100	173
Crystal system	Monoclinic	Monoclinic
Space group	$P2_1/c$	$P2_1/c$
Crystal size (mm^3)	0.53×0.14×0.09	0.53×0.14×0.09
a (Å)	9.4827(12)	9.6657(15)
b (Å)	9.6394(12)	9.6945(15)
c (Å)	26.754(3)	26.685(4)
β (°)	101.765(4)	102.793(5)
Volume (Å^3)	2394.1(5)	2438.4(6)
Z	4	4
$d_{calcd.}$ (g cm^{-3})	1.496	1.469
Reflections collected	12457	12617
Independent reflections	4543	4626
Parameters	317	317
R_1[a], wR_2[b] ($I > 2\sigma(I)$)	0.0841, 0.1971	0.0887, 0.2438
R_1[a], wR_2[b] (all data)	0.0925, 0.2031	0.1033, 0.2578
Goodness-of-fit on F^2	1.049	1.054

[a] $R_1 = \Sigma \, ||F_o| - |F_c|| \, / \, \Sigma \, |F_o|$.

[b] $wR_2 = [\, \Sigma \, w(F_o^2 - F_c^2)^2 \, / \, \Sigma \, w(F_o^2)^2 \,]^{1/2}$.

Table 7

Lattice constants of decamethylmetallocenium salts determined at –173 °C.

Compounds	Crystal system	a (Å)	b (Å)	c (Å)	β (°)	V (Å^3)
$[FeCp^*_2](C_4F_9SO_3)$	orthorhombic	12.274(4)	17.534(5)	13.025(4)	90	2803.0(5)
$[CoCp^*_2](C_4F_9SO_3)$	orthorhombic	12.097(5)	17.419(5)	13.094(5)	90	2754.9(17)
$[FeCp^*_2](C_8F_{17}SO_3)$	monoclinic	13.357(7)	13.655(7)	17.999(9)	93.48(2)	3213.2(3)
$[FeCp^*_2](C_4F_9CO_2)$	monoclinic	9.960(6)	9.462(6)	27.435(18)	97.98(7)	2704.0(2)

TOC

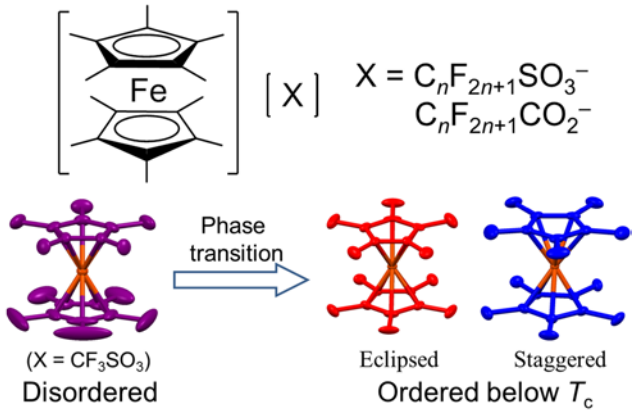
Fe
[X]
X = $C_nF_{2n+1}SO_3^-$
$C_nF_{2n+1}CO_2^-$
Phase transition
(X = CF_3SO_3)
Disordered
Eclipsed
Staggered
Ordered below T_c